Proc. Natl. Acad. Sci. USA
Vol. 76, No. 10, pp. 4760–4764, October 1979
Geophysics

Float trajectories in simple kinematic flows

(Lagrangian trajectories/float tracks/ocean currents)

LLOYD REGIER* AND HENRY STOMMEL

Woods Hole Oceanographic Institution, Woods Hole, Massachusetts 02543

Contributed by Henry M. Stommel, July 16, 1979

ABSTRACT **A simple kinematic model has been used to compute Lagrangian trajectories. Although it is certainly too simple to model geophysical flows, it has provided insights into the behavior of Lagrangian tracers. In particular, the existence of trapping regions has been shown to greatly increase the dispersion rate of tracers and to lead to net tracer displacements when the Eulerian mean flow is zero. In general, the spectrum of spatial scales present in the trajectories is wider than the Eulerian spectrum and is biased towards shorter wavelengths; the disparity between the 100-km Eulerian scale and the much shorter length scales experienced by the tracers is demonstrated. The estimation of the Eulerian parameters of the field from Lagranian observations must be done with a great deal of care, particularly if the eddy flow velocities are comparable to or exceed the mean flow. With a limited number of tracers it is extremely difficult to estimate, with any degree of confidence, the properties of either the mean Eulerian flow or the eddy field. Clearly, more effort must be spent to better understand the behavior of tracers in more realistic flows, to devise data analysis techniques, and to relate the Eulerian and Lagrangian spectra.**

Increased use of floats, balloons, and surface drifters has raised questions concerning the use and interpretation of such data for oceanographic and meteorological purposes. The analysis of Lagrangian data is complicated by two factors. First, it is extremely difficult to construct a truly Lagrangian tracer. Thus, the trajectory of a realizable quasi-Lagrangian instrument will in general differ from that of the fluid parcel allegedly being traced. Second, fluid flow fields historically have been studied, both theoretically and experimentally, from the Eulerian point of view. Although a Lagrangian description is in some sense a more natural way to examine the physics of fluid motion, our almost complete lack of experience with this method restricts our ability to interpret Lagrangian observations.

Perhaps as a result of this inexperience the tendency of most investigators has been to analyze Lagrangian data in terms of Eulerian constructs. For example, floats and drifters have been employed to obtain maps of large and mesoscale circulations even though it is well known that a fluid streamline and the trajectory of a fluid parcel coincide only for the simple case of nondivergent steady flow. Although it is possible, in principle, to relate the Eulerian and Lagrangian descriptions of a flow analytically, it must be noted that in general the Eulerian specification of the *entire* flow is required to compute the Lagrangian description, and conversely. Consequently, the transformation between the two descriptions cannot be performed for any realizable experiment. One extremely important issue that remains to be resolved is the extent to which one is capable of describing a flow field from the trajectories of a limited number of quasi-Lagrangian tracers.

We have attempted to familiarize ourselves with some of the characteristics of the trajectories of perfect Lagrangian tracers in some extremely simple patterns of kinematic motions. It is not our intention to provide a model that, by variation of its parameters, could be used to analyze a particular set of observations. Indeed, the model is far too simple to allow its application to the real world. Rather it is our intent to present a series of case studies which demonstrate some of the peculiarities of Lagrangian data as well as some of the dangers inherent in applying Eulerian analysis constructs to a finite amount of Lagrangian data. As will be seen, reliance on one's intuition can lead to misleading and totally false conclusions.

The model

We choose as our basic flow field the nondivergent flow described by the stream function

$$\psi(x,y,t) = \frac{A}{l}\cos l(x - c_x t)\cos l(y - c_y t) - u_0 y + v_0 x,$$

where x and y denote coordinates in a fixed frame of reference. This describes a flow that is the sum of a constant velocity (u_0,v_0) and a system of square cells or eddies of side length π/l, whose sense of rotation alternates from cell to cell in the sense of a checkerboard. The whole pattern moves with phase speed (c_x,c_y). The flow velocities at a fixed point are

$$u(x,y,t) = A\cos l(x - c_x t)\sin l(y - c_y t) + u_0 \quad \text{and}$$

$$v(x,y,t) = -A\sin l(x - c_x t)\cos l(y - c_y t) + v_0;$$

A is the peak amplitude of the eddylike motion.

When viewed from a reference frame x',y' moving at the phase velocity c_x,c_y relative to the fixed x,y frame, the stream function ψ' is steady and is given by

$$\psi'(x',y') = \frac{A}{l}\cos lx'\cos ly' - (u_0 - c_x)y' + (v_0 - c_y)x'.$$

It can be shown that there exist regions in x',y' bounded by closed contours of ψ' whenever

$$\left|\frac{u_0 - c_x}{A}\right| + \left|\frac{v_0 - c_y}{A}\right| < 1.$$

Because fluid parcels can never cross streamlines in this model, a tracer placed in a region so bounded is trapped within it and is seen in the fixed frame to propagate (with some perturbations due to motion within the trapping region) at the phase velocity. These trapping regions have a profound effect on tracer trajectories and have been described earlier by Stommel (1) and Flierl (2). Fig. 1 shows the fraction of the fluid contained within trapping regions as a function of the relevant parameters of the model.

In the case studies described below, a fourth-order Runge–Kutta method was used to numerically determine the tracer trajectories for various launch positions and different values of the parameters A, c_x, c_y, u_0, v_0; in all cases the eddy length scale was chosen to be $\pi/l = 100$ km, in keeping with the scale of

The publication costs of this article were defrayed in part by page charge payment. This article must therefore be hereby marked "*advertisement*" in accordance with 18 U. S. C. §1734 solely to indicate this fact.

* Now at Scripps Institution of Oceanography, La Jolla, CA 92093.

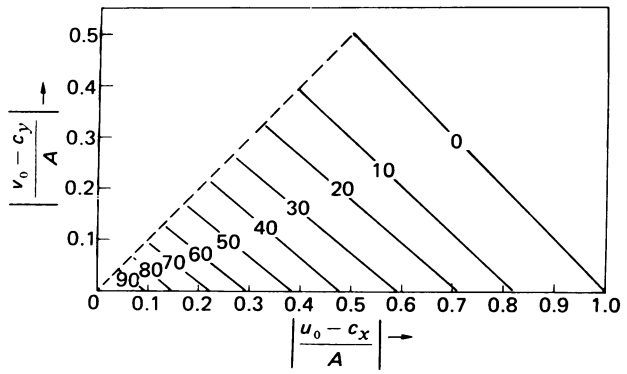

FIG. 1. Percentage of fluid contained within trapping regions. The diagram is symmetric about the diagonal.

mesoscale eddies. The tracers used are ideal in the sense that there is either no slippage of fluid past the tracer or the slippage is exactly known.

Time-independent flow

When $c_x = c_y = 0$, the Eulerian field is independent of time and the particle trajectories are particularly simple because they coincide with the streamlines of the flow. The simplest case results when $u_0 = v_0 = 0$, the trajectories being circles with slightly squared corners centered on the eddy cell center. The orbital period of a tracer depends on its initial distance from the eddy center, being $2\pi/lA$ for tracers launched near the center and tending towards infinity as the launch position approaches the edge of the cell. The Lagrangian velocity is zero near the center and increases to A at the cell wall, except the velocity is zero at the exact corner of an eddy cell. Thus, a set of tracers initially deployed along the x axis is distorted with time into the squared spiral shown in Fig. 2. There is no dispersion of tracers in the sense that a tracer will always remain in the cell in which it was launched, as may be seen in Fig. 1 which indicates that 100% of the flow is within the trapping region if $c_x - u_0 = c_y - v_0 = 0$.

If the Eulerian mean velocity u_0,v_0 is allowed to deviate from zero, the fraction of fluid trapped is diminished and some tracers may, depending on their launch position, migrate from cell to cell. Tracers within trapping regions will oscillate about but will eventually return to their initial position.

Time-dependent flow

Rather more interesting trajectories result if the flow field is allowed to propagate at phase velocity c_x,c_y. The Eulerian field is no longer steady and has a spectrum consisting of lines at angular frequencies $\omega = l|c_x + c_y|$ and $\omega = l|c_x - c_y|$. The trajectories of fluid particles are correspondingly more complicated, and, as might be expected from inspection of Fig. 1, their nature is strongly dependent on the relative sizes of A, $|c_x - u_0|$, and $|c_y - v_0|$. Unless expressly stated otherwise, $u_0 = v_0 = 0$ in the examples to follow.

Phase propagation parallel to cell wall

We now explore three examples in which the phase velocity is parallel to the eddy wall; in particular, we set $c_y = 0$. The examples differ in the size of the trapping region.

The first case has no trapped region and results from $c_x/A = 2$. Fig. 3 shows the stream function seen moving at the phase velocity. A tracer moving along a streamline experiences displacements parallel to the y' axis. Furthermore, because the y' spacing of streamlines does not remain constant, the x' component of velocity varies and the tracer is seen in the fixed frame to move slower or faster than the phase velocity. The trajectories

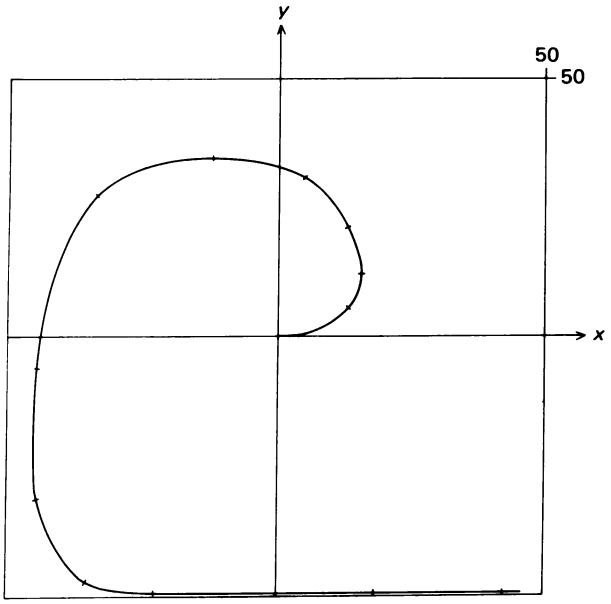

FIG. 2. Position after 10 days of a line of tracers originally launched along $y = 0$, $x = 0$ to 50 km in a stationary cell 100 km on a side with eddy amplitude $A = 20$ km/day.

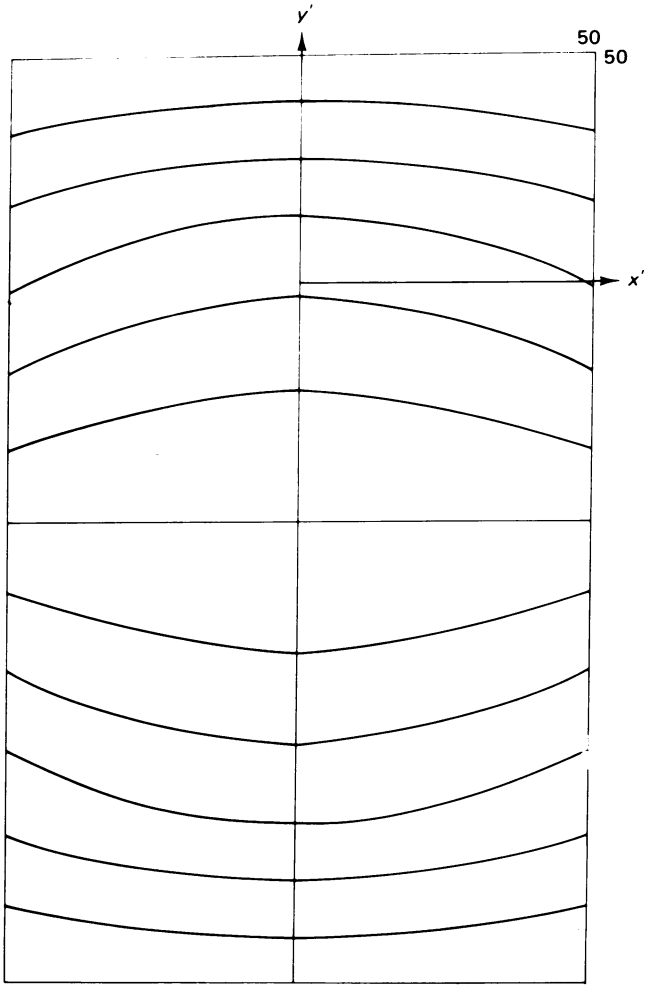

FIG. 3. Transport function seen moving with the eddy phase velocity for $A/|c_x| = 0.5$, $c_y = 0$, and $A = 5$ km/day.

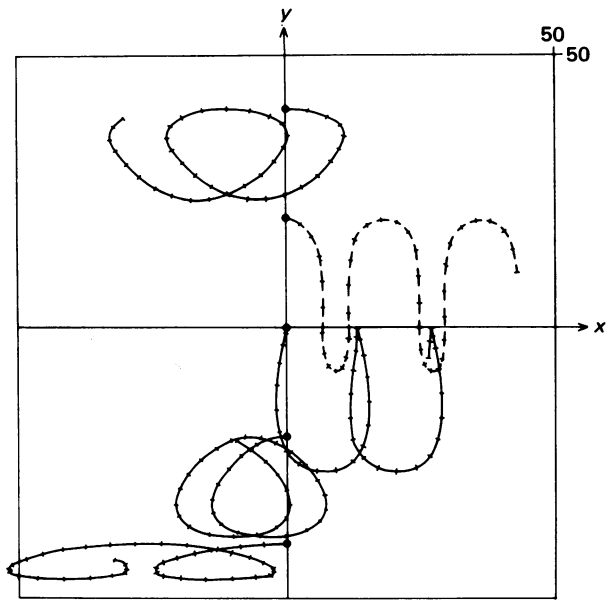

FIG. 4. Trajectories of tracers placed in the flow of Fig. 3. ●, Original launch points.

of five tracers relative to the fixed frame x,y are shown in Fig. 4, in which the tracer positions at 1-day intervals are marked by tics on the trajectory. The 100-km scale of the flow field is shown by the box. It is clearly apparent that the Lagrangian length scales are appreciably shorter than the Eulerian scale. Furthermore, the Lagrangian scale depends upon the launch point of the tracer. The nature of the trajectories is highly variable, with looping curves for those launched near the cell walls and serpentine curves dominating the interior.

It should be noted that the Eulerian mean flow is everywhere zero, whereas the Lagrangian tracers clearly exhibit long-term drifts with flows toward $+x$ in the interior and towards $-x$ nearer the cell wall. This apparent rectification is closely related to the Stokes drift of particles in linear surface waves. In fact, if $A/c_x \ll 1$, an expression can be derived for the long-term drift rate of tracers. We do not dwell on this further because the drift rate thus obtained vanishes completely if c_x and c_y are both nonzero.

When $c_x/A = 0.5$, trapping regions occupy about 40% of the fluid. This is clearly seen in Fig. 5 which shows the streamlines that move with the eddy. Also apparent in this figure are the extensive modulations of streamline spacing around the region of trapping. The effect this has on tracer trajectories may be seen in Fig. 6. The three tracers launched below the x axis are in the trapped region and propagate towards $-x$ in the direction of the phase velocity. The three trapped tracers have different length scales, none of which reflects the Eulerian scale. The two tracers launched at $+y$ have a net drift towards $+x$, again with length scales different from the Eulerian. If one were to estimate the mean Eulerian flow from these tracers, it is not likely that one would conclude the mean flow is everywhere zero.

The confusion of trajectories in Fig. 6 is greatly diminished if it is converted to a series of maps of quasi-Eulerian velocities obtained from the average velocity of each tracer between sequential fixes of its position. The eddy pattern and shear structure are clearly evident in the first frame of Fig. 7. In the succeeding frames the pattern becomes less clear as the tracers are dispersed across cell boundaries, but one can discern that on days 6 and 7 tracers 1 and 2 are in a counterclockwise rotating eddy to the right of the clockwise eddy containing tracers

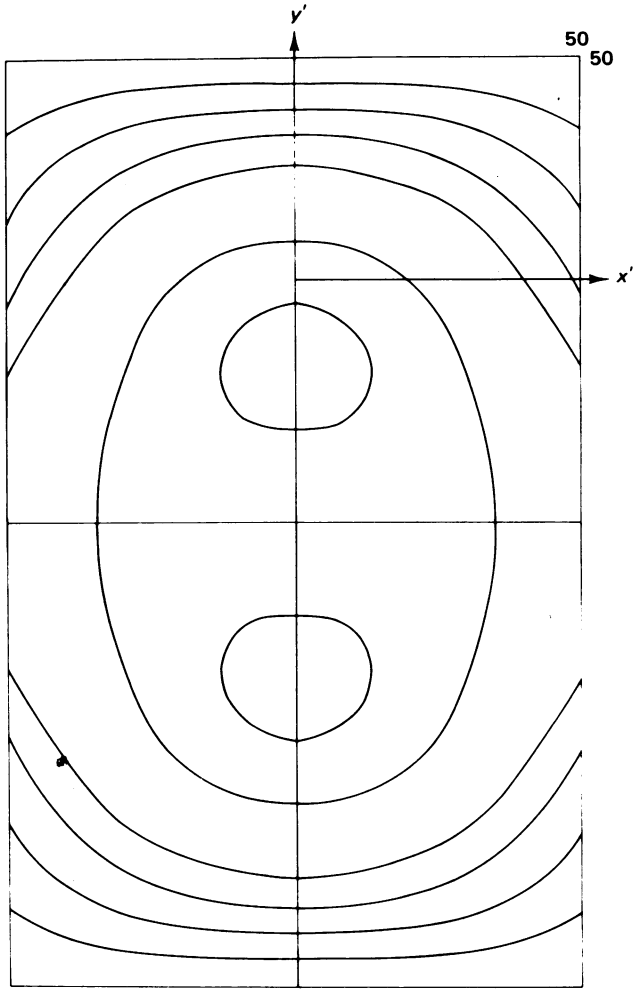

FIG. 5. Transport function seen moving with the phase velocity for A = 20 km/day and $A/|c_x|$ = 2, showing the trapping region.

3, 4, and 5. However, these quasi-Eulerian maps do not reveal the existence of the trapping region, the lack of a mean flow, or the phase velocity of the eddy pattern.

The third case study has 100% of the fluid trapped, which results when $c_x = u_0$. As shown in Fig. 8, the trajectories are cycloidal in nature with some modifications due to shearing within a cell. The Lagrangian length scales are once again dependent upon the initial distance from the eddy center, as are the orbital periods and velocities. If the tracer displacement is averaged over many orbital periods, a fairly good estimate of the mean velocity results because all tracers move at the phase speed with some perturbations due to orbital motion. However, the case of 100% trapping seems to be the only case for which the Eulerian mean can so easily be estimated.

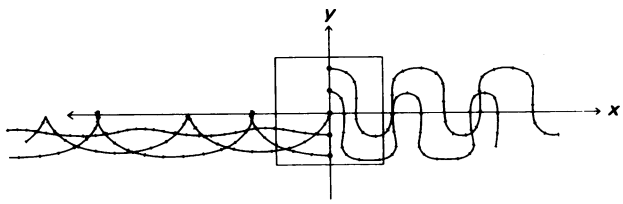

FIG. 6. Thirty-day trajectories of tracers placed in the flow of Fig. 5.

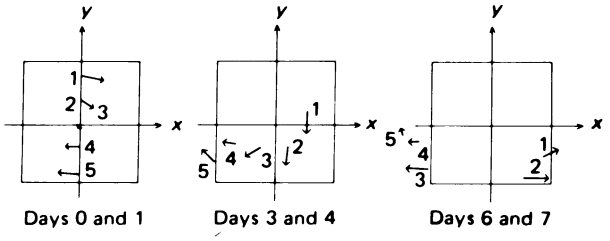

FIG. 7. Snapshots of distances traveled between successive fixes of tracer position in Fig. 6, which provides a quasi-Eulerian map.

Off-axis phase propagation

As implied in the discussion of the Stokes drift, the cases of phase propagation parallel to cell walls is rather special. We now examine several aspects of a case in which $c_x = -10$ km/day, $c_y = -2$ km/day, $A = 20$ km/day, and $u_0 = v_0 = 0$. Referring to Fig. 1, we found that 26% of the fluid is within trapping regions.

The trajectories of three tracers shown in Fig. 9 exhibit the behavior noted earlier. The tracer launched at the eddy center is in a trapping region and drifts to the left along a cycloidal path. The other two tracers are outside the trapping region and move off to the right in the direction opposite to the phase velocity. The appearance of cusps in their tracks as they cross cell borders is reminiscent of features found in actual trajectories of surface drifters (which have occasionally been attributed to the loss of the drogue).

The dispersion of a deployment of eight tracers placed on the periphery of a cell and one at cell center is traced in the quasi-Eulerian presentation of Fig. 10. A grid of the known cell size has been superimposed to show that the initial deployment has rapidly dispersed so that the tracers occupy five cells after only 10 days. This figure also shows that the quasi-Eulerian approach can help unravel some of the Eulerian parameters, but the task would be much more difficult if one did not know that the Eulerian field was periodic, had square cells of 100 km in length, and was propagating with the known phase velocity. The rapid dispersion of tracers limits the utility of maps of quasi-Eulerian velocities to short times after deployment of the array.

In attempts to minimize the dispersion of tracers, some experimentalists have used deployments of tracers in small clusters. Similar arrays have been used to obtain estimates of differential dynamic quantities, such as vorticity and horizontal divergence. In Fig. 11 are shown the initial and final positions of two clusters of tracers. Both clusters are initially 10 km in diameter and contain nine tracers each. The two clusters were launched simultaneously within 35 km of each other. After 20 days the cluster labeled R,P has moved 200 km along $-x$ and 20 km along $+y$ and has rotated about 240° clockwise; the cluster diameter and the relative position of tracers within the cluster remain unchanged. From this cluster one would infer a mean flow of (−20, 2) km/day and would conclude that the flow is nondivergent and in solid clockwise rotation.

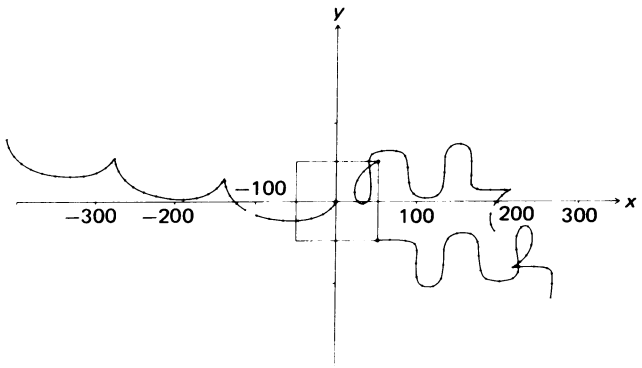

FIG. 9. Forty-day trajectories of three tracers in west by north-propagating eddies with $c_x = -10$, $c_y = 2$, and $A = 20$ km/day.

The small cluster labeled A,C suffers quite a different fate. After 20 days the cluster has been stretched to a length of 250 km and the relative position of tracers within the cluster was almost completely destroyed. One would conclude from this that the flow is perhaps turbulent and divergent and that the mean flow is (2.5, −4) km/day. The conclusions likely to be reached from separate consideration of each cluster are in error, and one can hardly speculate what conclusion might be reached from consideration of the trajectories of both clusters. And yet, all the tracers were launched within 35 km of each other in a flow whose single Eulerian length scale is 100 km.

The reason for this seemingly bizarre behavior is found in Fig. 12, which shows the stream function that moves with the phase velocity; the initial positions of the two clusters are also shown. The R,P cluster was placed in the center of a trapping region and thus moves at the phase velocity and can never get any larger than the stream function contour surrounding it. The A,C cluster, on the other hand, was by chance launched at the high-gradient region immediately adjacent to the trapping region. The length scales seen in this figure are very much shorter than the 100-km Eulerian scale, and this accounts for the rapid dispersal of the A,C cluster and the disparity between the behavior of the two clusters.

We have seen that the existence of trapping regions plays a

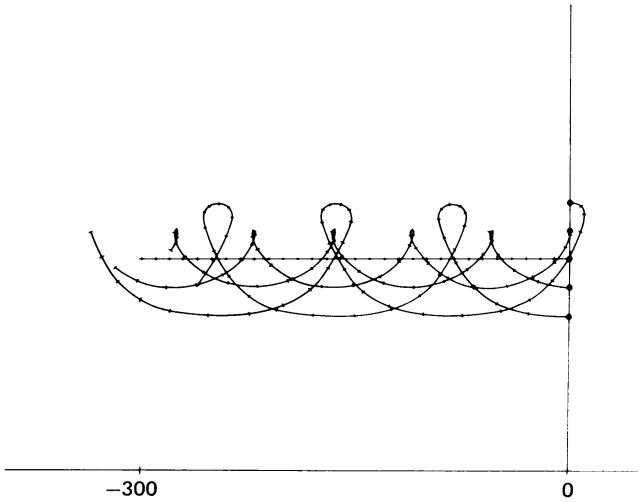

FIG. 8. Trajectories of tracers in the frozen eddy resulting when $c_x = u_0 = -10$ km/day.

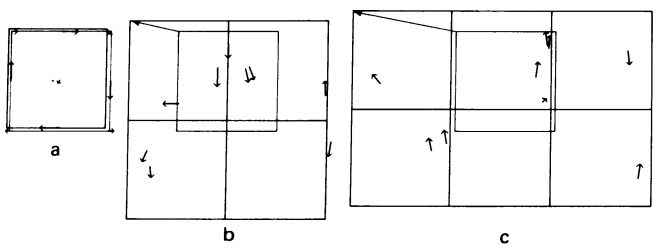

FIG. 10. Snapshot maps of quasi-Eulerian velocities obtained from nine tracers in the flow of Fig. 9. Instantaneous positions of cell walls have been superimposed to show the dispersal of tracers over five cells after 10 days.

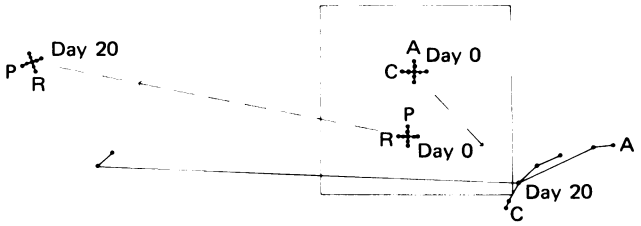

FIG. 11. Two small clusters placed in the flow of Fig. 9. The R,P cluster is within a trapping region and moves at the phase velocity with nearly simple rotation. The second cluster A,C is greatly deformed by day 20.

fundamental role in the dispersion of tracers. Those tracers that happen to be placed within a trapping region move at the phase velocity, whereas those outside the trapping region are advected in the opposite direction, dodging oncoming trapped regions

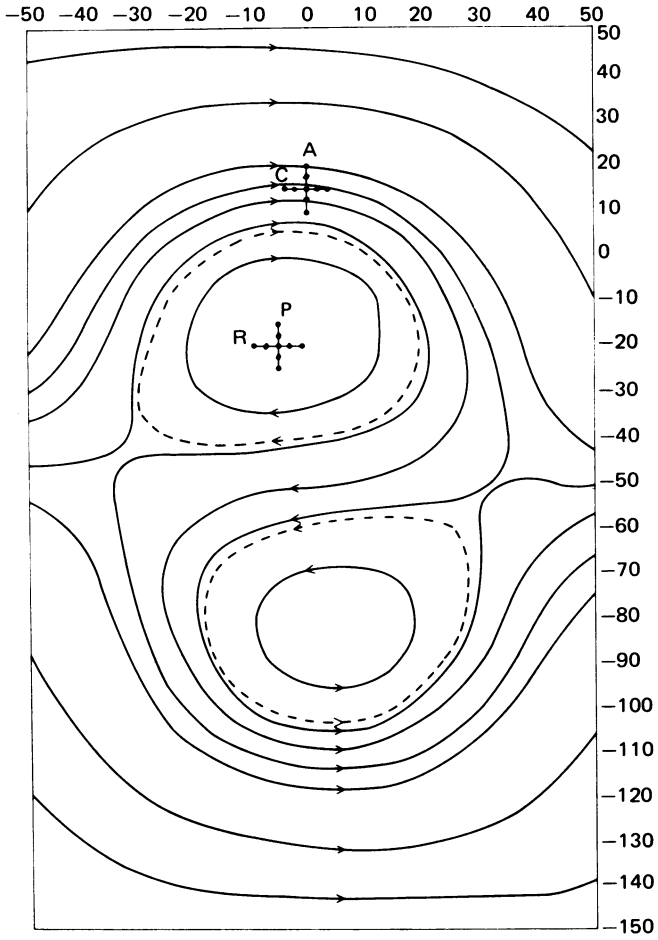

FIG. 12. Transport function seen moving at the phase velocity for the case of Fig. 9, showing the original positions of clusters traced in Fig. 11.

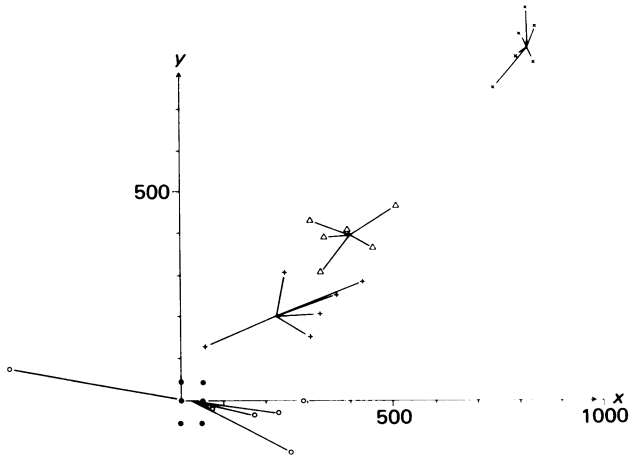

FIG. 13. Influence of mean (or self-propulsion) velocity u_0,v_0 on the dispersion of a cluster of six tracers: initial (●) and final positions for u_0,v_0 = 0,0 (○); 5,5 (+); 10,10 (△); and 20,20 (×) km/day.

as they go. Neither trapped nor untrapped tracers give a good indication of the mean velocity. It is reasonable to inquire whether there is some way to have a tracer visit both trapping and untrapping regions and thus have a net displacement more representative of the Eulerian mean. Reference to Fig. 1 reveals that if u_0,v_0 are made sufficiently large compared to A then the trapping region vanishes.

It is interesting that there are two mathematically equivalent interpretations of u_0,v_0. The first is that u_0,v_0 represents the constant Eulerian mean flow velocity. However, it can equally well be viewed as the slippage velocity between the tracer and the fluid parcel it is supposedly tracking. Thus, in light of this second interpretation, if the slippage of the tracer is known and can be made large enough, trapping regions cease to exist. In Fig. 13 the dispersion of a cluster of tracers is shown as the slippage u_0,v_0 increases from (0,0) to (20,20) km/day in a flow with A = 20 km/day. It is evident that the dispersion becomes less as the slippage is increased, which allows a more precise estimate of the sum of the true Eulerian mean and the tracer slippage velocities. If the slippage can be measured sufficiently accurately, a powered tracer may be a way to obtain meaningful estimates of the Eulerian mean current.

We are indebted to Mrs. Mary Hunt for parts of the programming used in this investigation. The work was carried out under National Science Foundation Grant OCE77-15600 to the Massachusetts Institute of Technology, but the actual study was undertaken at the Woods Hole Oceanographic Institution and its computing facility. It is Contribution No. 4361 of the Woods Hole Oceanographic Institution.

1. Stommel, H. (1950) *J. Mar. Res.* 8 (1), 24–29.
2. Flierl, G. (1976) *POLYMODE News*, 8, 1–9.